Defect-induced bandgap narrowing in low-k dielectrics

X. Guo, H. Zheng, S. W. King, V. V. Afanas'ev, M. R. Baklanov, J.-F. de Marneffe, Y. Nishi, and J. L. Shohet

Articles you may be interested in

Effects of vacuum ultraviolet irradiation on trapped charges and leakage currents of low-k organosilicate dielectrics
Appl. Phys. Lett. **106**, 192905 (2015); 10.1063/1.4921271

Valence and conduction band offsets at low-k a-SiOxCy:H/a-SiCxNy:H interfaces
J. Appl. Phys. **116**, 113703 (2014); 10.1063/1.4895135
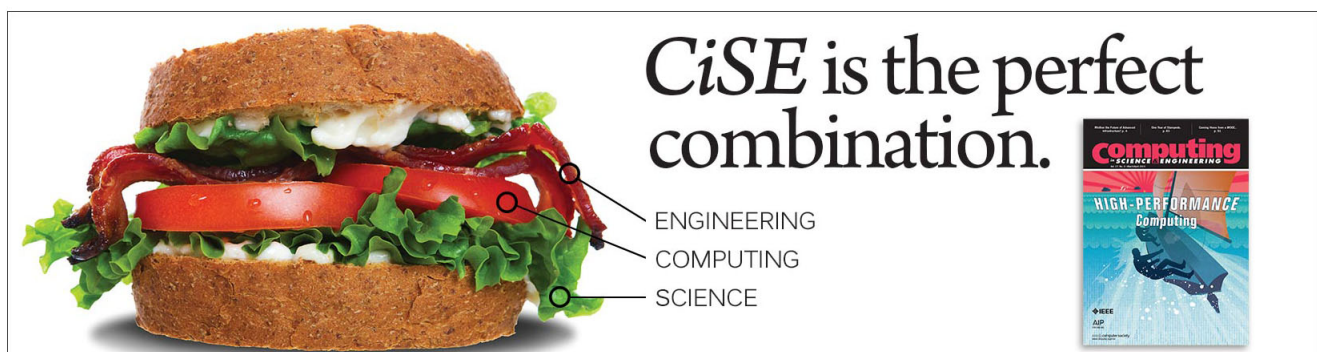
Measurement of bandgap energies in low-k organosilicates
J. Appl. Phys. **115**, 094105 (2014); 10.1063/1.4867644

Bandgap measurements of low-k porous organosilicate dielectrics using vacuum ultraviolet irradiation
Appl. Phys. Lett. **104**, 062904 (2014); 10.1063/1.4865407

Influence of electron-beam and ultraviolet treatments on low- k porous dielectrics
J. Appl. Phys. **100**, 124106 (2006); 10.1063/1.2401055

Defect-induced bandgap narrowing in low-k dielectrics

X. Guo,[1] H. Zheng,[1] S. W. King,[2] V. V. Afanas'ev,[3] M. R. Baklanov,[4] J.-F. de Marneffe,[4] Y. Nishi,[5] and J. L. Shohet[1]

[1]*Plasma Processing & Technology Laboratory and Department of Electrical and Computer Engineering, University of Wisconsin-Madison, Madison, Wisconsin 53706, USA*
[2]*Logic Technology Development, Intel Corporation, Hillsboro, Oregon 97124, USA*
[3]*Department of Physics, University of Leuven, B-3001 Leuven, Belgium*
[4]*IMEC, Kapeldreef 75, B-3001 Leuven, Belgium*
[5]*Department of Electrical Engineering, Stanford University, Stanford, California 94305, USA*

In this work, core-level X-ray photoelectron spectroscopy was utilized to determine the surface bandgap for various porous and non-porous low-k a-SiCOH dielectrics before and after ion sputtering. By examining the onset of inelastic energy loss in O 1s core-level spectra, the gap narrowing was universally found in Ar^+ ion sputtered low-k dielectrics. The reduction of the bandgap ranges from 1.3 to 2.2 eV depending on the film composition. We show that the bandgap narrowing in these low-k dielectrics is caused by development of the valence-band tail as evidenced by the presence of additional electronic states above the valence-band maximum. Electron-spin-resonance measurements were made on a-SiCOH films to gain atomic insight into the nature of the sputtering-induced defects and reveal formation of carbon-related defects as the most probable origin of the gap states. © 2015 AIP Publishing LLC. [http://dx.doi.org/10.1063/1.4929702]

Electrical reliability in Cu interconnect structures, such as stress-induced leakage currents, dielectric-breakdown voltages, and time-dependent dielectric breakdown (TDDB) failures, has become of vital concern as the nano-electronics industry moves to sub-16 nm and beyond technology nodes and strives to implement interlayer dielectric (ILD) materials with increasingly lower dielectric constants (i.e., low-k).[1–3] These reliability issues are typically attributed to the presence and creation of electrical "traps" or "defects" from porogen removal and plasma-etching processes that expose the material to intense ultraviolet (UV) and vacuum UV (VUV) photons, energetic ions, and chemically active radicals.[4–7] Numerous electrically based measurements have shown a direct correlation between trap/defect states, leakage current, breakdown voltages, and TDDB failures of low-k materials.[3,8,9] In most cases, the conduction mechanisms in dielectric materials are fundamentally dependent on accurate knowledge of the depths and locations of trap states within the bandgap. While due to the loss of translational symmetry of electronic states, there is no "true" bandgap for these amorphous low-k dielectrics. For understanding the energy positions of the defects as well as the possible conduction mechanisms in the materials, a number of empirical measurements have recently been devoted to determine the effective bandgap energy and to delineate the location of extended gap/defect states of the low-k dielectrics.[10–12]

While in most cases, the creation of defects and vacancies within the bandgap will cause a reduction of the bandgap by formation of additional electronic states either above the valence band or below the conduction band that overlap with one of these bands. For example, a conduction-band tail state may arise and extend below the conduction-band minimum (CBM) with the presence of vacancies and defect centers near the conduction band edge, or the valence-band maximum (VBM) may uplift due to an excess of electronic states originating nearby from disorder and imperfection of the materials. Both of these can lead a decrease in the bandgap. A number of electron-spin-resonance (ESR) measurements of porous/non-porous low-k dielectrics have shown that defects within these materials are silicon dangling bonds, neutral or positively charged oxygen vacancies and carbon residues,[13–15] all of which give deep states near the mid bandgap.[16] In addition, the Si-Si dangling bond can generate a bonding state in the lower gap and an antibonding state near the CBM. Oxygen vacancies possess a "shallow" bound state 1–2 eV below the CBM, while non-bridging oxygen can introduce states just above the VBM.[16] The effects of these additional electronic states on the experimental bandgap of low-k dielectrics are largely unknown and thus a more fundamental knowledge of the bandgap energy of the low-k dielectrics with intrinsic and/or post processing induced defect centers is needed. Considering this, an examination and comparison of the surface bandgaps were conducted on various a-SiCOH thin films before and after *in-situ* Ar+ sputtering, to investigate the band-gap narrowing phenomenon in low-k dielectrics.

Table I summaries some of the key properties for the low-k a-SiCOH thin films under study. Additional details concerning the film fabrication process and property measurements have been previously reported.[17,18] As can be seen, the a-SiCOH materials examined involve various compositions and dielectric constants that are representative of ILDs currently utilized or being considered for future applications. After the films were produced, X-ray photoelectron spectroscopy (XPS) measurements were made on the surface using a micro-focused monochromatic Al Kα X-ray source with a centroid photon energy of 1486.6 eV. During the measurement, a flood gun, which can generate a combination of low energy electrons (0.1 to 5.0 eV) and low energy Ar^+ ions, was used to neutralize any charge that built up at the surface

TABLE I. Summary of properties for a-SiCOH thin films investigated in this study. (PECVD = Plasma-enhanced chemical-vapor deposition, OS = Organosilane, AOS = Alkoxysilane, and EB = Electron beam.)

Film #	Deposition and precursor	Porogen	Cure	k-value (± 0.1)	Density (g/cm^3)	Porosity (%)	% Si	% O	% C	% H
1	PECVD-OS	No	No	3.3	1.5 ± 0.1	0	20.3	30.4	15.5	30.2
2	PECVD-AOS	Yes	EB	2.5	1.3 ± 0.1	25	16.9	29.2	18.2	35.8
3	PECVD-AOS	Yes	EB	2.2	1.1 ± 0.1	34	15.6	25.4	22.1	36.9

during the photoelectron emission process, or static charge from handling prior to analysis. Spectra were collected with a collection angle of 60° relative to the surface normal. The pass energy of the analyzer was set as 21 eV with a corresponding absolute resolution less than 0.5 eV. The depth of information depends on the material properties and the inelastic mean free path (IMFP) of electrons that usually varies with the element analyzed. For Al Kα x-ray activated O 1s photoelectron, the corresponding inelastic mean free path (λ_p) in SiO$_2$-like oxides is approximately 30–40 Å. According to the Beer-Lambert law,[19] 95% of the signal obtained with XPS originates from within three attenuation lengths of the surface (3 λ_p), which gives a sampling depth of 45–60 Å for a 60° electron exit angle. Each sample was measured 10 times and for each measurement the spectrum was scanned 50 times. Then, the bandgap energy of the sample was examined by extrapolating a linear fit to the leading edge of the electron energy-loss spectrum and by locating the onset of inelastic energy loss relative to the core-level peak.[11,12] The accuracy of this method can be ~0.5 eV or less if the electron density in the valence band near surface is laterally homogeneous and the largest source of error is due to uncertainty in the process of linear extrapolation.[11] A more reliable and accurate procedure might be obtained by using a fitting law of the form $(E-E_g)^n$ ($n = 1/2$ for direct bandgap and $n = 3/2$ for indirect bandgap materials).[20,21] After that, a 4 keV Ar$^+$ ion-sputtering beam, from the monatomic argon ion sources equipped in the same analyzing chamber, was utilized *in-situ* to create defects on the sample surface.[12] The ion beam current was 15 μA/cm^2 and the sputtering time was 30 s. XPS measurements with the same procedure were then performed on the ion-sputtered spot of the sample to get a comparison to the bandgap energy before and after ion sputtering.

Figure 1 shows the inelastic-loss spectra near the O 1s core-level peak collected from a 100 nm a-SiCOH film (k = 3.3) before and after *in-situ* Ar$^+$ ion sputtering, which had been calibrated with reference to the C 1s peak at 284.8 eV. The location of the O 1s core-level peak was determined to be 532.6 eV. To see how the sputtering-induced charging affects the uniformity of the potential distribution across the oxide surface, the full width at half maximum (FWHM) of the O 1s peak was also examined on each sample. No comparable broadening of the O 1s emission line was observed after ion sputtering. By tracking the intersection of the leading edge (*solid straight line*) and the background level (*dashed horizontal line*) of the electron energy inelastic loss spectra, as shown in Figure 1, the onset of inelastic losses was found to occur at 540.7 eV for the pristine samples. To quantify the uncertainties of the linear extrapolation, least-square-fitting regression lines with 95% confidence were constructed (*dotted straight lines*) to the

inelastic loss peak leading edge, by which the errors of the linear extrapolations were estimated to be ± 0.3 eV with 95% confidence. According to these analyses, the bandgap of pristine a-SiCOH film (k = 3.3) was calculated to be 8.1 ± 0.3 eV by subtracting the binding energy of O 1s peak at 532.6 eV from that of onset of inelastic losses. This value agrees with the reported bandgap energy of 8.2 eV for a-SiCOH film (k = 3.3) measured by reflection electron energy loss spectroscopy (REELS).[12] Similarly, the bandgap of the sample after ion sputtering was calculated to be 6.8 ± 0.3 eV. It should be mentioned that the spectra of ion-sputtered a-SiCOH does not show the oxygen-vacancy defects as previously observed with REELS.[12] One possible reason can be the difference of the sampling depth between these two works: the REELS spectra, using 500 eV electron excitation beam, mainly originate from the topmost 7–10 Å, while the depth of information for the O 1s core-level peak obtained by XPS in this work is approximately 45–60 Å. The damage depth in SiO$_2$-like dielectrics by Ar$^+$ ion sputtering under 4 keV is larger than 20 Å, depending on the film density and composition. Thus, the detected O 1s photoelectrons in this work are believed to come from the ion-damaged layer and the unperturbed bulk underneath.

Table II shows the bandgap measurements on all of the samples. As can be seen, after 4 keV ion-beam sputtering, the bandgap energies of the a-SiCOH films were all reduced. The reduction ranges from 1.3 eV to 2.2 eV depending on the film composition. These reductions cannot be ascribed to measurement errors alone and suggest that additional states must have been created within the bandgap. Thus, valence-band XPS measurements were made to examine the valence-band density of states of each sample. By linearly fitting to the rising edge of the spectra, as shown in Figure 2(a), the
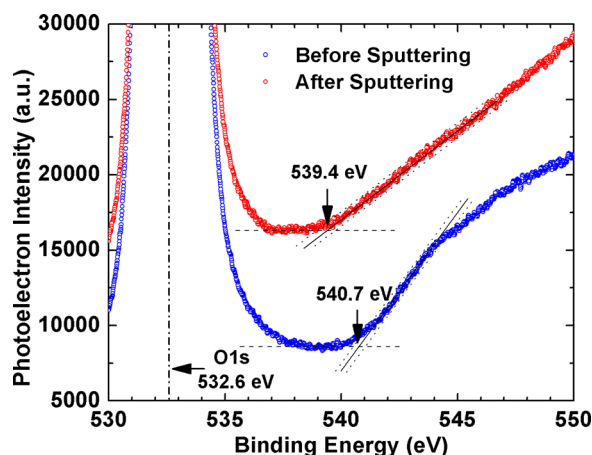

FIG. 1. Bandgap measurements of a-SiCOH (k = 3.3) film before and after ion sputtering by linearly fitting to electron energy loss spectra with 95% confidence interval.

TABLE II. Summary of bandgap energy and valence band position before and after ion sputtering for the a-SiCOH films under study. It should be noted that, to keep consistent to Figure 2(a), the VBE positions here are all referred to the Fermi level, and larger values correspond to deeper band edges.

Film #	Before ion sputtering		After ion sputtering	
	Bandgap (±0.3 ev)	VBE (±0.1 ev)	Bandgap (±0.3 ev)	VBE (±0.1 ev)
1	8.1	4.1	6.8	2.8
2	8.0	4.0	6.2	2.2
3	8.3	4.2	6.1	2.0

FIG. 3. ESR signals measured on a-SiCOH (k = 3.3) film before and after ion sputtering.

valence-band edge (VBE) of the pristine a-SiCOH film was determined to be approximately 4.1 eV. For the ion-sputtered sample, however, additional electronic states were detected above the VBM, as illustrated by the arrow, resulting in a shift of the VBE towards to 2.8 eV. Since no broadening was observed for the FWHM of the O 1s peak after sputtering, the apparent "tail" of the electron-energy distribution must originate from the sputtering-induced defects, rather than any local fluctuations of electrostatic potential across the film surface caused by sputtering. A schematic representation of the density of states is depicted in Figure 2(b), to show the changes of band structures after ion sputtering. One can see that in the ion-sputtered sample, a valence band tail appears and extends above the VBM. The up-shifting of VBE was calculated to be 1.3 eV by subtracting the VBE value of ion-sputtered sample from that of pristine sample, which is in excellent agreement with the bandgap reduction, suggesting that the bandgap narrowing after sputtering must be attributed to the uplifting of valence band.

To obtain insight into the nature of defects generated during ion sputtering, ESR measurements were carried out on a-SiCOH thin films deposited on high-resistivity silicon wafers. Figure 3 shows the conventional first-derivative absorption spectra of the ESR signal from the samples with the applied magnetic field **B** parallel with the sample surface. The values of the g-factor and the linewidth of the defect center were determined by fitting the spectra into the Lorentzian derivative line shape using least squares. Control spectra were measured on the pristine sample and were observed to exhibit signals only originating from silicon dangling bonds. These silicon dangling-bond defects (generally known as P_{b0} and/or P_{b1} centers), similar to the bulk E' centers, are usually from the underlying a-SiCOH/Si interface
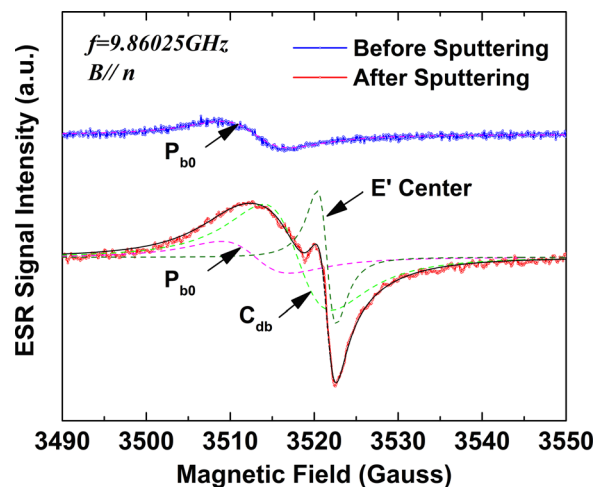
with no measurable density of paramagnetic defects pertaining to the low-k dielectric layer itself.[22,23] However, after ion sputtering, the intensity of P_{b0}/P_{b1} increased. Actually, splitting off H from a Si-H bond in the oxide results in the same signal as E' but in the neutral state.[24] In the shown case of non-porous chemical-vapor deposition (CVD) oxide, this may happen simply because of electron-hole pair generation and hole trapping on the Si-H bonds.[25] It should be noticed that, while observed by ESR measurement, the core-level photoemission spectra on ion-sputtered sample do not show the existence of silicon dangling-bonds. Besides the difference of core-level XPS information depth as discussed earlier, another possible reason might be the low density of the silicon dangling-bonds within the film, as evidenced by the low intensity of P_{b0} peak in ESR spectra. In addition to that, peaks with much higher intensity emerged in the ESR spectra. The predominant peak is characterized with a g-factor of 2.0006 and a linewidth of 2 G. These have been attributed to surface oxygen vacancies (SOV), in which the defects were usually positively charged in the paramagnetic state.[15] The other signal at g = 2.0026 with an approximate linewidth of 7 G is identified as due to carbon-dangling-bonds (C_{db}) back-bonded to C or Si atoms.[14]

These observations are consistent with the ESR results reported by previous authors that ion sputtering-induced defects in low-k dielectrics are oxygen/silicon vacancies analogous to the oxygen-deficient centers/silicon dangling bond centers in bulk SiO_2 and carbon-dangling-bonds from
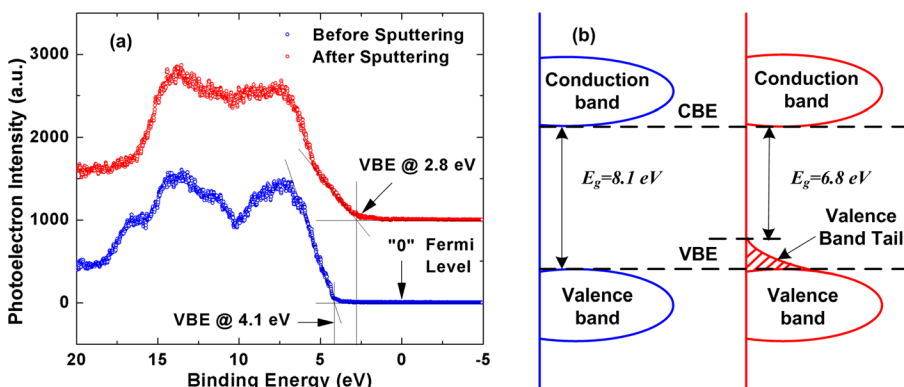

FIG. 2. (a) Valence band XPS spectra of a-SiCOH (k = 3.3) film before and after ion sputtering, where the "0" binding energy corresponds to the energy of the Fermi level. (b) Schematic representation of the density of states of a-SiCOH (k = 3.3) film before and after ion sputtering.

carbon silicide cluster in the material.[14,15] The SOV has been previously identified as a defect that creates sub-gap surface defects at $\approx$5.0 and 7.2 eV,[12] which are in the upper half of the bandgap and close to the CBM. The silicon dangling bounds possess a highly localized state near the mid-bandgap, lying near the isolated sp^3 or p hybrid energies, which will not contribute to the states below the Fermi level either.[16] As a result, the states near VBM must originate from sputtering induced carbon-related defects, which had been shown to give rise to "deep" energy levels near the VBE of the SiO_2-like skeleton in a low-k dielectric material.[26,27] Usually, the excessive carbon-dangling bonds at the interfaces result in electron states distributed in the lower half of the oxide bandgap.[26] In addition, electron states associated with a-C:H layers can be found in the same energy range.[27] It is also likely that our ESR experiments detect only the fraction of the sputtering-induced defects with an unpaired electron while diamagnetic entities escape ESR detection. Nevertheless, the Si carbide and oxycarbide clusters generally represent the most stable bonding configurations and may be produced by ion sputtering in densities sufficient to cause the revealed formation of the VB "tail."

To conclude, core-level XPS measurements have been utilized to measure the bandgap energy of low-k a-SiCOH films before and after Ar^+ ion sputtering. The results show that bandgap narrowing occurs in ion-sputtered a-SiCOH films and the reduction of bandgap varies with the film composition. Valence-band XPS measurements show that additional electron states are created near the VBE by ion sputtering and the bandgap reduction originates from the tail extended above the VBM. Further ESR examination reveals that the carbon dangling-bond defects are responsible for measured bandgap narrowing. These observations suggest that the defects within the bandgap of the low-k dielectric films are largely responsible for electrical degrading and likely limit the dielectric reliability.

[1]J. Lloyd, E. Liniger, and T. Shaw, J. Appl. Phys. **98**, 84109 (2005).
[2]J. Atkin, E. Cartier, T. Shaw, J. Lloyd, R. Laibowitz, and T. Heinz, Microelectron. Eng. **86**, 1891 (2009).
[3]M. Nichols, H. Sinha, C. Wiltbank, G. Antonelli, Y. Nishi, and J. Shohet, Appl. Phys. Lett. **100**, 112905 (2012).
[4]F. Chen and M. Shinovsky, IEEE Trans. Electron Devices **56**, 2 (2009).
[5]K. Tanbara and Y. Kamigaki. J. Electrochem. Soc. **157**, G95 (2010).
[6]X. Guo, J. E. Jakes, S. Banna, Y. Nishi, and J. L. Shohet, J. Appl. Phys. **116**, 044103 (2014).
[7]X. Guo, S. W. King, H. Zheng, P. Xue, Y. Nishi, and J. L. Shohet, Appl. Phys. Lett. **106**, 012904 (2015).
[8]B. Bittel, P. Lenahan, and S. King, Appl. Phys. Lett. **97**, 63506 (2010).
[9]J. Atkin, D. Song, T. Shaw, E. Cartier, R. Laibowitz, and T. Heinz, J. Appl. Phys. **103**, 94104 (2008).
[10]A. Grill, J. Appl. Phys. **93**, 1785 (2003).
[11]M. T. Nichols, W. Li, D. Pei, G. A. Antonelli, Q. Lin, S. Banna, Y. Nishi, and J. L. Shohet, J. Appl. Phys. **115**, 094105 (2014).
[12]S. W. King, B. French, and E. Mays, J. Appl. Phys. **113**, 044109 (2013).
[13]H. Ren, M. T. Nichols, G. Jiang, G. A. Antonelli, Y. Nishi, and J. L. Shohet, Appl. Phys. Lett. **98**, 102903 (2011).
[14]V. V. Afanas'ev, A. P. D. Nguyen, M. Houssa, A. Stesmans, Zs. Tokei, and M. R. Baklanov, Appl. Phys. Lett. **102**, 172908 (2013).
[15]T. A. Pomorski, B. C. Bittel, P. M. Lenahan, E. Mays, C. Ege, J. Bielefeld, D. Michalak, and S. W. King, J. Appl. Phys. **115**, 234508 (2014).
[16]E. P. O'Reilly and J. Roberson, Phys. Rev. B **27**, 3780 (1983).
[17]S. King, R. Chu, G. Xu, and J. Huening, Thin Solid Films **518**, 4898 (2010).
[18]S. King, D. Jacob, D. Vanleuven, B. Colvin, J. Kelly, M. French, J. Bielefeld, D. Dutta, M. Liu, and D. Gidley, ECS J. Solid State Sci. Technol. **1**, N115 (2012).
[19]R. Cammack, T. Atwood, P. Campbell, H. Parish, A. Smith, F. Vella, and J. Stirling, *Oxford Dictionary of Biochemistry and Molecular Biology*, 2nd ed. (Oxford, 2008).
[20]J. Rafferty and L. M. Brown, Phys. Rev. B **58**, 10326 (1998).
[21]M. C. Cheyneta, S. Pokranta, F. D. Tichelaar, and J.-L. Rouvière, J. Appl. Phys. **101**, 054101 (2007).
[22]J. Thomas and S. Hofmann, J. Vac. Sci. Technol., A **3**, 1921 (1985).
[23]E. Paparazzo, J. Phys. D: Appl. Phys. **20**, 1091 (1987).
[24]V. V. Afanas'ev and A. Stesmans, J. Phys.: Condens. Matter **12**, 2285 (2000).
[25]S. Shamuilia, V. V. Afanas'ev, P. Somers, A. Stesmans, Y.-L. Li, Zs. Tőkei, G. Groeseneken, and K. Maex, Appl. Phys. Lett. **89**, 202909 (2006).
[26]V. V. Afanas'ev, M. Bassler, G. Pensl, M. Schulz, and E. Stein von Kamienski, J. Appl. Phys. **79**, 3108 (1996).
[27]V. V. Afanas'ev, A. Stesmans, and M. O. Andersson, Phys. Rev. B **54**, 10820 (1996).